PERGAMON

Vision Research 39 (1999) 3662–3672

Vision Research

www.elsevier.com/locate/visres

Sensitivity and dynamics of rod signals in H1 horizontal cells of the macaque monkey retina.

J. Verweij [a,b], D.M. Dacey [a,*], B.B. Peterson [a], S.L. Buck [b]

[a] *Department of Biological Structure, The University of Washington, Box 357420, Seattle, WA 98195-7420, USA*
[b] *Department of Psychology, The University of Washington, Seattle, WA 98195, USA*

Received 7 September 1998; received in revised form 7 December 1998

Abstract

We measured the sensitivity, temporal frequency response, latency, and receptive field diameter of rod input to the H1 horizontal cell type in an in vitro preparation of the macaque retina. The H1 cell has both a cone-connected dendritic tree and a long axon-like process that terminates in a rod-connected arbor. We recorded from the H1 cell body where rod signals were distinguished by sensitivity to short wavelength light after dark adaptation. Receptive fields of rod vs. cone mediated responses were coextensive, indicating that the rod signal is transmitted via rod–cone gap junctions. Sensitivity of the H1 cell rod signal was ~1 log unit higher than that of the cone signal. Below cone threshold rod signals were temporally low-pass, with a cutoff frequency below 10 Hz. Rod signals became faster and more transient with increasing light levels. We conclude that the H1 cell rod signal is not sensitive in the low scotopic range and, by comparison with the rod signal recorded directly in cones (Schneeweis & Schnapf (1995) *Science*, *268*, 1053–1056), signal transmission across the cone-H1 synapse does not significantly filter the temporal properties of the rod signal.

Keywords: Macaque; Rod; Cone; Horizontal cell; Sensitivity

1. Introduction

In human vision rod signals are transmitted by two mechanisms that differ in sensitivity and temporal resolution (Buck, 1989; Sharpe, Stockman, & MacLeod, 1989; Sharpe & Stockman, 1991). The duality in rod vision has been measured in observers without cone function (Hecht, Shlaer, Smith, Haig & Peskin, 1938, 1948; Hess & Nordby, 1986; Blakemore & Rushton, 1998) and in normal observers by stimulating rods in isolation (Conner & MacLeod, 1977; Conner, 1982; Knight & Buck, 1993). One of the rod mechanisms underlies lowest scotopic vision and cannot resolve temporal frequencies above 15 Hz. The other mechanism has a threshold about 3 log units higher—in the mesopic range—and can resolve temporal frequencies up to ~28 Hz (Conner & MacLeod, 1977). Both mechanisms must originate in the retina since they can be identified physiologically in the electroretinogram (Sharpe & Stockman, 1991; Stockman, Sharpe, Rüther, & Nordby, 1995).

The two rod mechanisms may originate in a dichotomy in the way mammalian retinal circuits transmit rod signals to ganglion cells (Kolb, 1970; Raviola & Gilula, 1973; Kolb & Famiglietti, 1974; Famiglietti & Kolb, 1975; Nelson, Kolb, Famiglietti, & Gouras, 1976; Nelson, 1977). In one of the pathways for rod signals in the retina—the rod bipolar pathway—rods synapse with rod bipolar cells which do not directly contact ganglion cells but instead direct output to a distinctive amacrine cell type, the AII. Output of the AII amacrine is mainly to ON cone bipolar cells via gap junctions (Strettoi, Dacheux & Raviola, 1994) and to OFF cone bipolar cells via an inhibitory synapse (Strettoi, Raviola, & Dacheux, 1992; Muller, Wässle, & Voigt, 1988); the AII cell thus provides a pathway by which rod signals can be transmitted via cone bipolar cells to both ON and OFF ganglion cell populations. Amacrine cells in the rod bipolar pathway respond to light in the scotopic range (Nelson, 1982; Nelson & Kolb, 1985),

* Corresponding author. Tel.: +1-206-543-0224; fax: +1-206-543-1524.
E-mail address: dmd@u.washington.edu (D.M. Dacey)

0042-6989/99/$ - see front matter
PII: S0042-6989(99)00093-0

suggesting that this pathway, at least, underlies the most sensitive rod mechanism observed in human vision. A second rod pathway bypasses the rod bipolar circuit and links rods directly to cones via gap junctions (Raviola & Gilula, 1973). Rod signals in the rod–cone pathway have been recorded in cones in cat (Nelson, 1977) and macaque monkey (Schneeweis & Schnapf, 1995), and in cone-driven horizontal cells in cat (Nelson et al., 1976; Nelson, 1977; Lankheet, Rowe, van Wezel & van de Grind, 1996a,b). This rod-cone pathway is relatively insensitive compared to the rod bipolar pathway (Smith, Freed & Sterling, 1986; Lankheet et al., 1996a), and in macaque the rod mediated pulse response recorded in cones speeds up and shows a transient component at higher light levels (Schneeweis & Schnapf, 1995). The rod–cone pathway therefore has at least some properties consistent with the less sensitive but faster human rod mechanism. A simple correspondence between retinal pathways and human mechanisms has been questioned, however, since both rod mechanisms are found in observers who may only have few or no cones (Sharpe & Stockman, 1991).

To further clarify the link between retinal circuitry and human rod vision it is necessary to characterize the rod pathways in primates. In this study we focused on the rod–cone pathway in the macaque retina. This rod signal is potentially accessible for recording in the L + M-cone driven H1 horizontal cells using an in vitro preparation of the intact retina (Dacey, Lee, Stafford, Pokorny, & Smith, 1996). A complication is that the H1 cells have two distinct anatomical components: a cone-connected dendritic tree and a rod-connected arbor that is tethered to the cone-connected tree via a long, thin axon-like process (Fig. 1a). Rod input recorded in the horizontal cell body however should be transmitted via the rod–cone gap junction since the cone- and rod-connected networks appear to function as electrotonically isolated independent units (Nelson, Lutzow, Kolb, & Gouras, 1975; Rodieck, 1988). Here we first identify a rod input to the H1 cell body and determine the sensitivity and the temporal characteristics of the rod signal. We further provide evidence that this signal is transmitted via rod–cone gap junctions by measuring the rod- and cone-mediated receptive fields.

2. Methods

2.1. In vitro preparation and histology

The in vitro preparation of macaque retina has been previously described (Dacey & Lee, 1994; Dacey et al., 1996; Stafford & Dacey, 1997). In brief, eyes were obtained from juvenile and adult *Macaca fascicularis* ($n = 2$), *M. nemestrina* ($n = 16$), *M. mulatta* ($n = 1$), and *Papio anubis* ($n = 1$) through the Tissue Distribution Program of the Regional Primate Research Center at the University of Washington. Whole eyes were removed under deep barbiturate anesthesia just prior to euthanasia. Retinas were dissected free of the vitreous and sclera in oxygenated culture medium (Ames' Medium, Sigma) and placed flat, vitreal surface up, in a superfusion chamber mounted on the stage of a light microscope. H1 cell nuclei were identified at the outer border of the inner nuclear layer (Fig. 1b) (Dacey et al., 1996) following a 30 min superfusion of the nuclear stain 4,6 diamidino-2-phenylindole (DAPI) (20 μM). For combined intracellular recording and staining, microelectrodes were filled with a solution of 2–3% Neurobiotin (Vector Labs., Burlingame, CA) and 1–2% pyranine (Molecular Probes, Eugene, OR) in 1M KCL. Electrical impedances ranged from 180 to 300 MΩ. Pyranine fluorescence in the electrode and DAPI fluorescence in cells were viewed together under episcopic illumination with the same filter combination. Penetration of the cell body was confirmed by iontophoresis of pyranine into the cell. Light responses were evaluated for stability and overall quality for about 15 min before gathering data.

After recording from a cell, the cell was ionotophoretically injected with Neurobiotin (+ 0.1–

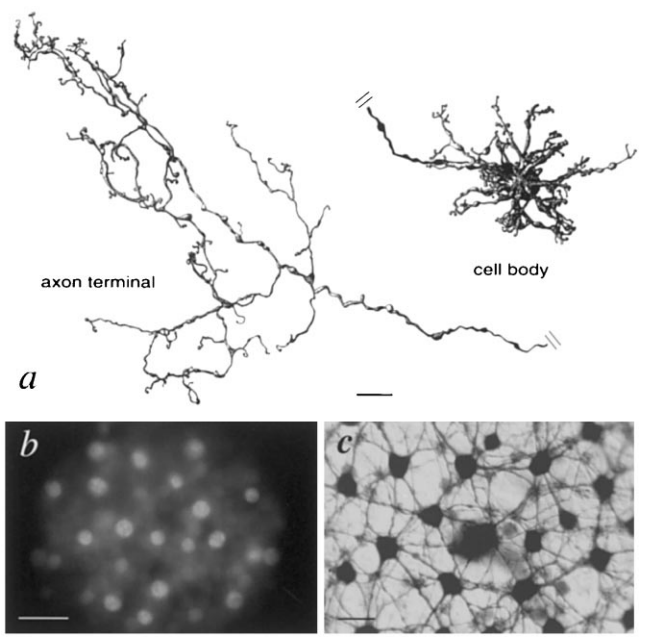

Fig. 1. (a) Camera lucida tracing of the cell body and axon terminal of a Golgi impregnated macaque H1 cell located 13 mm from the fovea. The axon (full length not shown) extended about 2 mm across the retina. Scale bar = 10 μm. (b) Photomicrograph of a flat mounted macaque retina showing the intensely fluorescing nuclei of horizontal cells stained with DAPI. (c) Photo-micrograph of a patch of the H1 cell mosaic revealed with intracellular injection of Neurobiotin into the center cell. Scale bars in b and c = 25 μm

0.2 nA; ~15 min). At the end of an experiment, retinas were dissected free of the choroid and fixed in phosphate buffered (0.1 M, pH 7.4) 4% paraformaldehyde for ~2 h then rinsed in 0.1 M phosphate buffer and placed in a buffered solution of 0.1% triton X-100 (Sigma) containing the Vector avidin-biotin-HRP complex (Vector Laboratories, Burlingame, CA) for 5 h or overnight. Retinas were rinsed for 2 h and standard HRP immunohistochemistry was performed using diaminobenzidine (DAB) (Kirkegaard & Perry Laboratories, Gaithersburg, MD) as the chromogen. Retinas were mounted on a slide in a water-based solution of polyvinyl alcohol and glycerol (Heimer & Taylor, 1974).

Macaque retinal tissue stained by the Golgi method was kindly donated by Bob Rodieck. Many H1 cells with completely impregnated dendritic arbors, axons, and terminal arbors were observed in this material, one of which was used to create the illustration in Fig. 1a.

2.2. Light stimulation and data acquisition

Light responses were recorded using a light emitting diode (LED) based stimulator (Dacey & Lee, 1994; Dacey et al., 1996). Light sources were red and blue LEDs (peak wavelengths 658 and 448 nm respectively; bandwidths 18 and 70 nm respectively) mounted on a small optical bench above the microscope such that the light path was projected through the camera port as a spot on the retinal surface. The spectral output of the LEDs was measured in the plane of the retina using a spectral radiometer (Gamma Scientific). The spectral efficiency of the red and blue LEDs for the long (L), middle (M), and short (S) wavelength sensitive cones and the rods was calculated using macaque cone and rod spectral sensitivity curves (Baylor, Nunn & Schnapf, 1987). Spectral sensitivity was corrected for self-screening assuming an axial pigment density of 0.05 for the L- and M-cones and 0.35 for rods (Baylor, Nunn & Schnapf, 1984, 1987). The spectral efficiency of the red LED for the L-, M-, and S-cones and rods was calculated to be, respectively, 1.1, 2.0, 6.4, and 3.2 log units less than for quanta at the optimal wavelength for the specific photoreceptor (L, 561 nm; M, 531 nm; S, 430 nm; rod, 491 nm). For the blue LED the respective values were 0.7, 0.4, 0.2, and 0.2 log units. Thus the red LED was most effective for stimulation of L- cones whereas the blue LED was highly effective but less specific for stimulation of rods. The irradiance of the stimuli was expressed as log quanta μm^{-2} s^{-1}. Although we recognize that the most accurate term for quantifying our light stimulus is irradiance, for the purpose of this paper we have adopted the more familiar and commonly used term 'intensity' in place of irradiance.

Light responses were recorded under conditions of both light and dark adaptation. Since H1 cells were penetrated using intense violet episcopic illumination, light adapted cone mediated responses were recorded first while the rods were still saturated. The relative intensities of the red and blue LEDs were adjusted to give equal H1 cell response amplitudes. Response sensitivities were determined using a 2 mm diameter spot stimulus modulated as a 400 ms pulse. Response latencies were measured with 10 ms pulses over the same ranges. The interstimulus interval in the light adapted retina (no rod input) was a minimum of 700 ms. In the dark adapted retina, the interstimulus interval was increased to 3 s to give time for recovery before the next flash; the reproducibility of the responses indicated that a 3 s interval was long enough to avoid significant adaptational effects. Temporal frequency responses were determined using sinusoidal modulation (0.61–52.1 Hz in 19 steps) around a mean level. The Michelson contrast (100% × amplitude/mean) of the stimulus was 100%. The receptive field profile of the cell was determined by projecting a temporally modulated square wave through a slit, forming a stimulus 2×170 μm at the retinal surface, and recording responses at nine positions in the cell's receptive field.

Retinas were dark adapted for ~30 min during which time the sensitivity to a weak stimulus was tested about every 5 min; sensitivity typically reached a maximum after ~25 min. Following dark adaptation the sensitivity, latency, temporal frequency response, and receptive field measurements were made for near threshold intensities of the red and blue LEDs. In order to limit the effects of stray light associated with high intensity stimuli, a slit stimulus set at about 1.5 log units above threshold was used for receptive field measurements.

Small differences in response amplitude were observed between the light and dark adapted cone responses to the red LED (Figs 2c and 5c) which we believe reflects some variability over time in the quality of our intracellular recordings. The difference, though small, implies that the cone component of the blue LED response may also have increased during dark adaptation and that the rod component of the response as estimated by our subtraction process (see Section 3 and Fig. 4) may be contaminated by a residual cone signal. Initially, we estimated the magnitude of the residual cone artifact from the difference responses to the red LED and scaled the cone responses to the blue LED accordingly in our subtraction process, with the result that the shape and size of the scaled and unscaled responses were virtually identical. This satisfied us that scaling was not necessary and that the cone response differences were very small and inconsequential to our analysis of the rod signal.

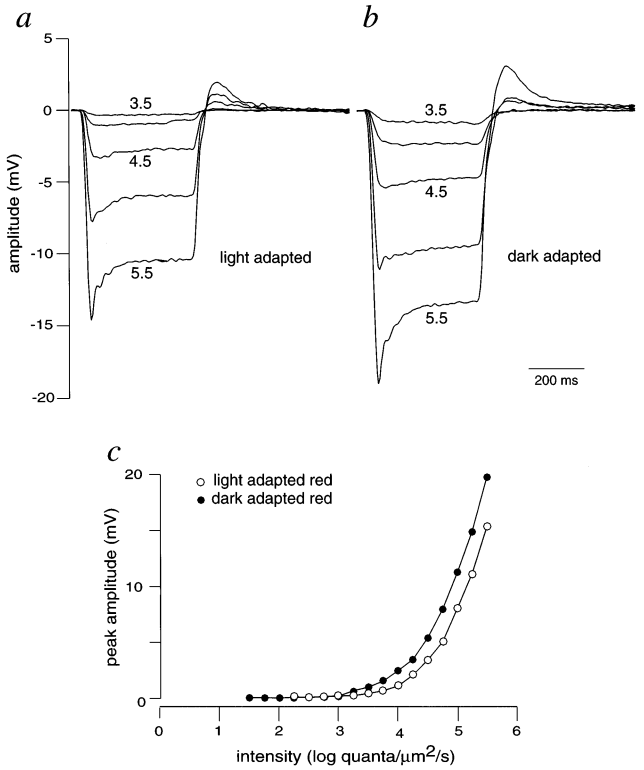

Fig. 2. H1 cell responses to the red LED in the light and dark adapted retina. (a) Responses of a light adapted H1 cell to 400 ms pulses of various intensities (steps of 0.5 log units). Numbers indicate the intensity of the stimulus in log quanta $\mu m^{-2}\ s^{-1}$. (b) Responses of the same cell to the same stimuli after 30 min of dark adaptation. (c) Peak responses of the same H1 cell, plotted as a function of the intensity of the red LED before (open symbols) and after (filled symbols) dark adaptation. (Data from a and b).

3. Results

3.1. Cell identification

The distinctive morphology of the H1 horizontal cell is illustrated in the camera lucida tracing of a Golgi impregnated macaque H1 cell shown in Fig. 1. The cell's dendritic terminals contact cone pedicles. The long, thin, axon-like process terminates in an arbor that contacts rod spherules. H1 cells in our preparation were reliably identified at the outer border of the inner nuclear layer by DAPI fluorescence (Dacey et al., 1996). The large nuclei of DAPI-fluorescing H1 cells are shown in Fig. 1b. Intracellular injection of the small tracer, Neurobiotin, reveals the coupled dendritic network of a population of H1 cells, as shown in the micrograph of Fig. 1c. The characteristic axon-like process of H1 cells could also be discerned but the HRP staining typically did not reveal the complete extent of the axon and the rod-contacting terminals.

3.2. Shape and size of rod input to H1 horizontal cells

Our basic strategy was to record the light adapted cone mediated response to red (most efficient for L-cones, inefficient for rods) and blue (most efficient for rods, less efficient for M- and L- cones) LED stimuli, then dark adapt the retina and record responses to the same stimuli. Using these two stimuli, we determined rod and cone contributions to the light response at light levels above cone threshold and also measured rod input below cone threshold after dark adaptation.

Responses of a light adapted H1 cell to 400 ms pulses of the red LED over a 2 log unit range are shown in Fig. 2a. Responses of the same cell to the same stimuli after 30 min of dark adaptation are shown in Fig. 2b. Fig. 2c shows response peak amplitudes plotted as a function of intensity for the light and dark adapted conditions. The magnitude of the effect of dark adaptation can be seen as a small shift along the intensity axis of about 0.25 log units in Fig. 2c. The small difference in response amplitude between the light and dark adapted conditions is probably due to the quality of the intracellular recordings, as discussed below (see Section 4).

Fig. 3 shows responses of the same cell to the blue LED under the same adaptation conditions. These responses were more strongly affected by dark adaptation than responses to the red stimulus. Four effects of dark adaptation are apparent in Fig. 3a and b. First, the sensitivity to dim stimuli was increased by about 1.8 log units in the dark adapted retina. Second, near-threshold responses in the dark adapted retina were much slower than in the light adapted retina. Third, responses to higher intensity stimuli in the dark adapted retina showed a more pronounced transient at light onset. And, fourth, the dark adapted near-threshold response to stimulus offset contained a slow component. Fig. 3c shows response peak amplitudes plotted as a function of intensity for the light and dark adapted conditions. The effect of dark adaptation on responses to the blue LED cannot be described by a simple shift of the light adapted curve along the intensity axis, as it was for dark adapted responses to the red LED (compare Figs 3c and 2c). Differences in the stimulus intensity that elicited a response of the same peak amplitude in the light and the dark adapted H1 cell were larger for near-threshold responses than for responses to higher intensity stimuli (Fig. 3c). The differences in H1 cell responses to the red and blue stimuli with dark adaptation are consistent with rod input responses observed in cat horizontal cells (Steinberg, 1969c; Nelson, 1977).

In Fig. 4 we estimated the rod contribution to dark adapted responses to the blue LED for the H1 cell shown in Fig. 3. Rod light offset responses are much slower than cone light offset responses (Steinberg, 1969b,c). Close to threshold, the dynamics of the offset

responses to the blue LED were consistent with rod but not with cone input. The intensity at which the cones start to contribute to the H1 cell response can be recognized by the appearance of a fast component in the offset response (Fig. 3b). Above this intensity we can only estimate the shape of the rod input. Our estimations were based on two assumptions: (1) rod and cone signals sum linearly; and (2) the cone mediated responses in light and dark adapted H1 cells are very similar. Fig. 4 shows the estimated rod responses for light levels at which the rod part of the response dominated. Since responses to intensities up to 1.9 log quanta $\mu m^{-2}\ s^{-1}$ were almost purely due to rod input, the responses to 0.4–1.9 log quanta $\mu m^{-2}\ s^{-1}$ in Fig. 4 are simply the dark adapted blue responses of the cell

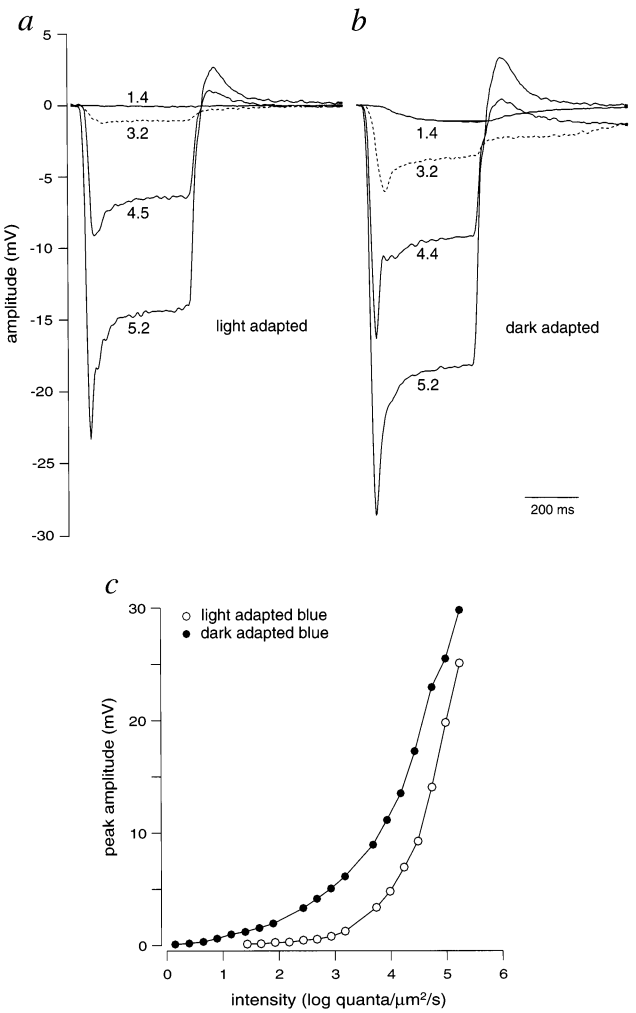

Fig. 3. H1 cell responses to the blue LED in the light and dark adapted retina (same cell as in Fig. 2). (a) Responses of a light adapted H1 cell to 400 ms pulses of various intensities. Numbers indicate the stimulus intensity in log quanta $\mu m^{-2}\ s^{-1}$. (b) Responses of the same cell to the same stimuli after 30 min of dark adaptation. (c) Peak response of the H1 cell versus the intensity of the blue LED before (open symbols) and after (filled symbols) dark adaptation. (Data from a and b).

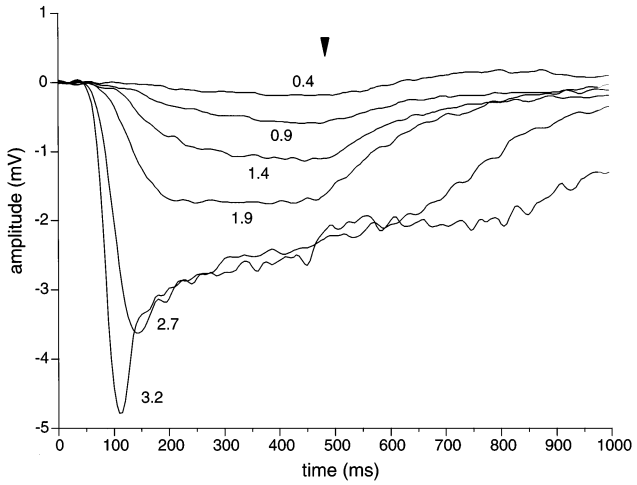

Fig. 4. Estimated rod contribution to the blue LED responses of the dark adapted H1 cell shown in Fig. 3. Stimuli were 400 ms pulses of varying intensities delivered 25 ms after beginning data acquisition. Since the dark adapted blue response was due almost entirely to rod input up to an intensity of 1.9 log quanta $\mu m^{-2}\ s^{-1}$, the four lowest intensity traces are simply the dark adapted blue response. At higher intensities (2.7 and 3.2 log quanta $\mu m^{-2}\ s^{-1}$), where cones began to contribute to the response, the cone contribution was subtracted out by subtracting the light adapted from the dark adapted response. Rod input sensitivity for the nine dark adapted cells shown in Table 1 were determined by taking the response amplitude 60 ms after the blue LED stimulus was turned off (arrowhead).

shown in Fig. 3. The size of the rod responses to 2.7 and 3.2 log quanta $\mu m^{-2}\ s^{-1}$, where cones began to contribute to the response, was estimated by subtracting the light adapted response from the dark adapted response. Fig. 4 shows that the rod mediated response in H1 cells has a shortened time to peak with increasing light levels. In contrast, the response offset slows down with increasing light levels. Similar results were found in 8 of the 10 H1 cells that were stimulated and analyzed in the same way. In the remaining two cells, the speeding up of the onset response was not clearly discernible.

3.3. Sensitivity of rod mediated H1 cell responses

The sensitivity of the dark adapted H1 cell to rod and cone input is shown in Table 1. Stimuli were 400 ms pulses of the red and blue LEDs. Rod input sensitivity was determined by measuring the response amplitude 60 ms after the blue stimulus was turned off (arrow in Fig. 4), when the amplitude of the rod response to dim stimuli was still very close to the peak response amplitude but the cone contribution was minimal. Sensitivity data for a cell were used only when the maximum amplitude of the rod mediated response was larger than 1.5 mV. Sensitivities shown in Table 1 are expressed as the ratio of response size in mV to stimulus intensity in equivalent 491 nm quanta $\mu m^{-2}\ s^{-1}$

(the wavelength to which rods are most sensitive) for the weakest stimulus that evoked a response amplitude of about 0.5 mV. The average sensitivity of the rod input to 9 H1 cells was 0.0849 ± 0.0474 mV per 491 nm quantum μm^{-2} s^{-1}. The average sensitivity of the three most sensitive H1 cells was 0.141 ± 0.030 mV per quantum μm^{-2} s^{-1}.

Sensitivity of the cone mediated response was determined using the peak response amplitude to the red LED for the weakest stimulus that evoked a response amplitude of about 0.5 mV (Table 1). Since H1 cell responses to our red stimulus were probably dominated by L-cone input (see Section 2), we calculated the spectral efficiency of the red LED relative to that of a 561 nm stimulus (wavelength of peak sensitivity for L-cones) (Baylor et al., 1987). The average sensitivity of the L-cone input to 9 H1 cells was 0.0034 ± 0.0013 mV per 561 nm quantum μm^{-2} s^{-1} (Table 1). The average sensitivity of the three most sensitive H1 cells was 0.0049 ± 0.0003 mV per 561 quantum μm^{-2} s^{-1}. Thus, on average, the sensitivity of rod input to dark adapted H1 cells was about 1.4 log units greater compared to the L-cone input.

3.4. Temporal characteristics of the rod response in H1 cells

3.4.1. Response latency

The peak latency of rod and cone mediated responses of light and dark adapted H1 cells was determined with 10 ms pulses of the blue and red LEDs (Fig. 5). Responses to the red LED were slightly larger in the dark adapted retina but peak latencies showed little if any difference. For example, peak latencies for the light and dark adapted responses shown in Fig. 5a and b were 30 and 35 ms respectively. In Fig. 5c, the light adapted responses to the red LED have been subtracted from the dark adapted responses. Peak latencies of the difference responses in Fig. 5c were about 40 ms for all stimulus intensities.

Responses of the same H1 cell to 10 ms pulses of the blue LED are shown in Fig. 5d and e. The peak latency of the light adapted responses was 30–35 ms for all intensities (Fig. 5d). Peak latencies of the dark adapted responses were 105, 85, 70, and 45 ms for pulse photon densities of 0.6, 1.1, 1.9, and 2.4 log quanta μm^{-2} respectively (Fig. 5e). We estimated the rod contribution to the dark adapted blue LED re-

Table 1
Sensitivity of dark adapted H1 cell rod and L-cone mediated responses

Cell	Sensitivity rod input (491 nm) (mV quantum^{-1} μm^{-2} s^{-1})[a]	Sensitivity L-cone input (561 nm) (mV quantum^{-1} μm^{-2} s^{-1})[b]	Sensitivity rod/cone input (log)
02/26/97.2	0.0200		
03/18/97.2	0.0656	0.0049	1.11
04/02/97.2	0.0582	0.0035	1.17
04/02/97.4	0.0334		
07/09/97.1	0.0933	0.0052	1.45
07/09/97.2	0.1209	0.0045	1.75
07/16/97.1		0.0036	
08/20/97.1	0.1827	0.0033	1.71
08/27/97.3	0.1185	0.0029	1.49
10/01/97.4	0.0714		
10/15/97.3		0.0012	
10/15/97.4		0.0018	
Average	0.0849	0.0034	1.40
Standard deviation	0.0474	0.0013	0.22

[a] Stimulus was 400 ms pulses of blue light of increasing intensity ($\sim$0.25 log units steps). Response amplitude was determined 60 ms after blue light was turned off, when the cone mediated responses have returned nearly to baseline but near the threshold rod responses are still close to maximum amplitude. Values are averages of 16 stimulus presentations. Sensitivity was corrected to the values that would have been obtained with monochromatic 491 nm light (wavelength of maximum sensitivity for rods). Our wideband blue light was less efficient in stimulating rods than a 491 nm light by a factor 1.5 (calculated using the rod spectral sensitivity curves as determined by Baylor et al. 1984; corrected for self-screening assuming an axial pigment density of 0.35).

[b] Cone mediated response sensitivity determined with red light. Methods were the same as for rod response sensitivity except that peak response amplitude was used. Since our red light was less effective for M-cones, H1 cell responses were probably dominated by input from L-cones (see Section 2). Sensitivity was corrected to values that would have been obtained with a 561 nm stimulus (wavelength of maximum sensitivity for L-cones) and assuming an axial pigment density of 0.05 for L-cones.

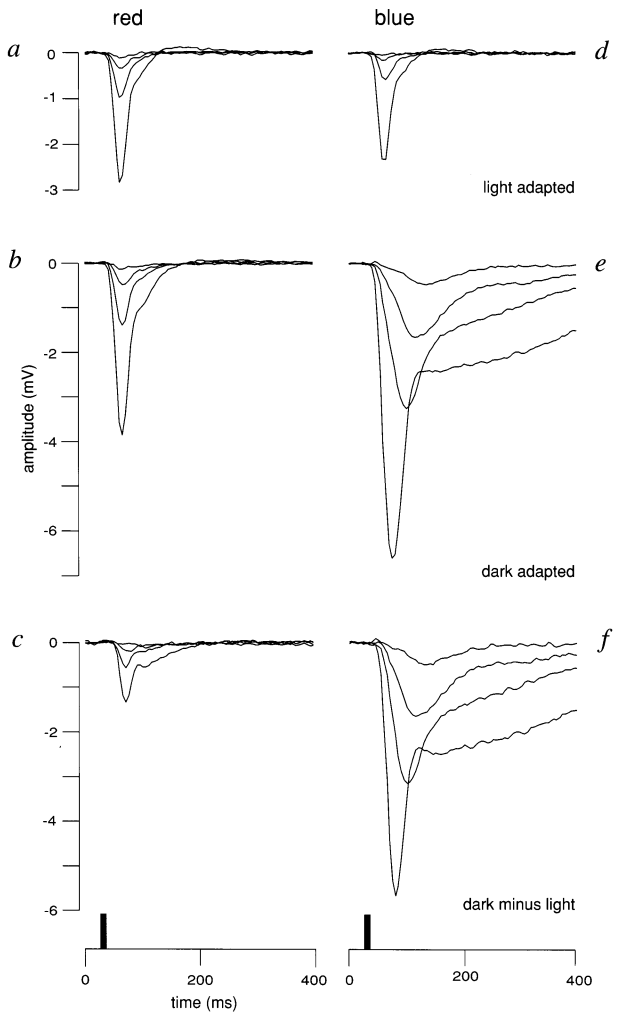

Fig. 5. Responses of an H1 cell to 10 ms pulses of the red and blue LEDs. Pulse duration is indicated by the vertical bars at the bottom of the traces. (a) Light adapted responses to the red LED stimulus (pulse photon densities were 1.6, 2.1, 2.6, and 3.1 log quanta μm^{-2}). (b) Responses of the same cell to the same stimuli after dark adaptation. (c) Linear subtraction of responses in a from responses in b. (d) Light adapted responses of the same cell to the blue LED (pulse photon densities were 0.6, 1.1, 1.9, and 2.4 log quanta μm^{-2}). (e) Responses to the same stimuli after dark adaptation. (f) Linear subtraction of responses in d from responses in e.

sponse by subtracting light adapted from dark adapted responses (Fig. 5f). The corresponding peak latencies of the difference responses (estimated rod responses) were 105, 85, 70, and 50 ms for pulse photon densities of 0.6, 1.1, 1.9, and 2.4 log quanta μm^{-2} respectively. Similar results were found in all three cells that were tested with the same protocol; the time to peak of dark adapted blue LED responses in H1 cells decreased with stimulus intensity from 105–165 ms, for an intensity of about 2.6 log quanta $\mu m^{-2}\ s^{-1}$, to about 45–55 ms for an intensity of 4.4 log quanta $\mu m^{-2}\ s^{-1}$.

3.4.2. Temporal frequency response

We determined the temporal resolution of dark adapted H1 cells using sinusoidally modulated red and blue LEDs with a Michelson contrast of 100% (Fig. 6). Threshold responses to the red stimulus were obtained with an average stimulus intensity of about 2.7 log quanta $\mu m^{-2}\ s^{-1}$. The amplitude of the response to the red stimulus increased steeply over a 3 log unit range in intensity from threshold to 5.8 log quanta $\mu m^{-2}\ s^{-1}$ (Fig. 6a). The frequency of the red stimulus at which the response fell to 10% of peak amplitude (cutoff frequency) increased with stimulus intensity from about 25 Hz for stimuli near threshold to about 50 Hz for stimuli 3 log units above threshold (Fig. 6a).

For the blue LED, the range in stimulus intensity from threshold to a maximum response amplitude was more than 4.5 log units (Fig. 6b). The shape of the temporal frequency responses for intensities of 3.0 log quanta $\mu m^{-2}\ s^{-1}$ and higher were very similar to those of equal amplitude red LED responses and had similar cutoff frequencies, indicating they were dominated by cone input. The amplitude of the blue light response

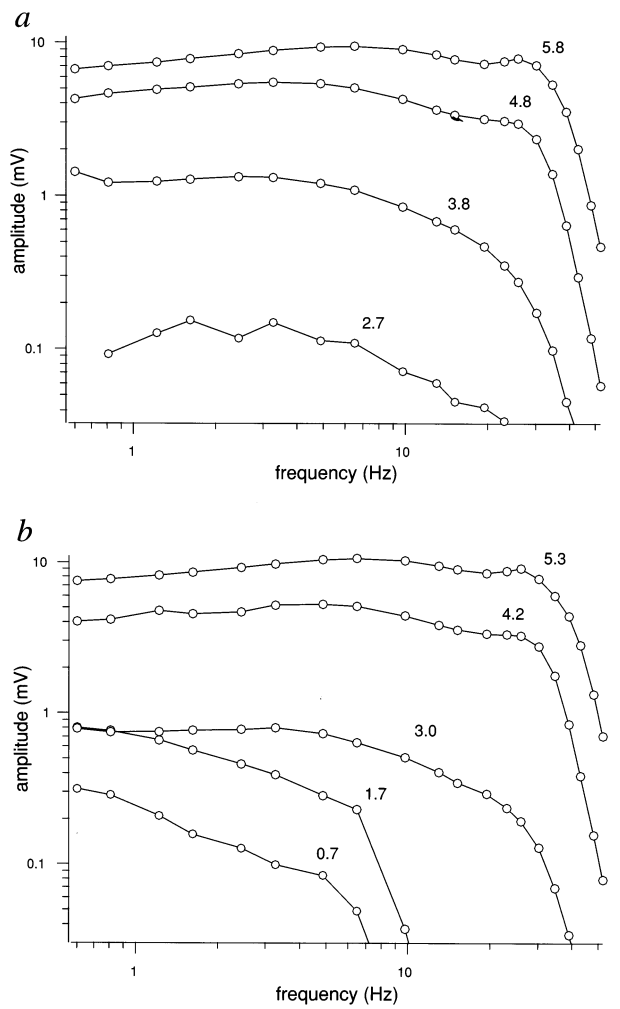

Fig. 6. Temporal frequency response curves of a dark adapted H1 cell for various intensities of sinusoidally modulated (modulation depth = 100%) red (a) and blue (b) LED stimuli. Numbers next to traces give the stimulus intensity in log quanta $\mu m^{-2}\ s^{-1}$.

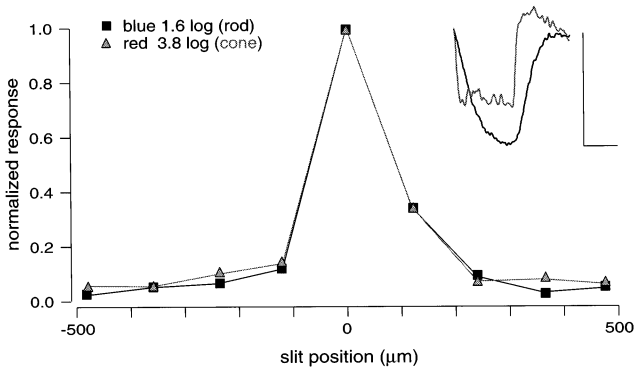

Fig. 7. Receptive field profiles of cone (△) and rod (□) signals in a dark adapted H1 cell. The red (△) and blue (□) LED stimuli were projected as slits 170 μm wide and 2 mm long and delivered as 400 ms flashes at nine positions in the receptive field. Stimulus intensity was chosen such that cone input dominated the red LED response and rod input dominated the blue LED response. Responses were normalized relative to the response to a centered slit. Responses to the centered slit stimuli are shown in the inset (blue stimulus, bold line; red stimulus, thin line; verticle scale bar = 1 mV; horizontal scale bar = 500 ms).

did not increase with light level for intensities between 1.7 and 3.0 log quanta μm^{-2} s^{-1}. For intensities at or below threshold for cone input (1.7 and 0.7 log quanta μm^{-2} s^{-1}), responses were relatively large and had a lower cutoff frequency; the response amplitude fell to 10% of peak amplitude at frequencies below 10 Hz (Fig. 6b). Similar results were found in 16 of 17 cells tested using this protocol. For higher light levels—above cone threshold—the rod mediated temporal frequency response could not be determined because the cone mediated response was large relative to the smaller rod mediated signal.

3.5. Receptive fields of cone and rod input into H1 cells

To test the hypothesis that rod input in H1 cells is due to rod-cone coupling and not to input transmitted via the H1 cell's rod-contacting axon-like process, we measured rod and cone mediated receptive fields of H1 cells (Fig. 7). We reasoned that if rod signals were transmitted over millimeters of retina to reach the H1 cell body, this would give rise to a mismatch in receptive field location and size for rod versus cone input. For receptive field measurements the intensity of the blue stimulus was about at threshold for cone input, generating a rod dominated response, while the intensity of the red stimulus was chosen such that it elicited a cone-mediated response of about equal amplitude. Responses shown in Fig. 7 were normalized relative to the response to a centered slit. Rod and cone mediated receptive field profiles were nearly identical. The inset to Fig. 7 shows the cone mediated response to the red stimulus and the rod mediated response to the blue stimulus for slit stimuli presented in the center of the receptive field. The receptive fields of four additional H1 cells also had rod-mediated and cone-mediated receptive fields matched in location and size.

4. Discussion

4.1. Identification and origin of rod signals in H1 cells

The light response of H1 cells to our red and blue stimuli under light and dark adapted conditions revealed a clear rod input. First, dark adaptation resulted in a large increase in the response amplitude of H1 cells to the rod-efficient blue stimuli but not to the cone-efficient red stimuli (Figs 2c and 3c). A small difference in response amplitude between the light and dark adapted responses to the red LED (Figs 2c and 5c) was often observed. This would not be expected on the basis of predicted rod or cone sensitivity to the red LED. We believe it reflects a small variability over time in the quality of our intracellular recordings. For example, a recording will typically improve, and response amplitude increase, during about the first 20 min following penetration. For this reason alone the dark adapted cone mediated light responses will usually not perfectly match the light adapted responses. This implies that the rod components computed by subtraction may contain a small contaminating cone component. Regardless of the small amplitude differences for the light and dark adapted red LED conditions, however, the very large dark adapted increase in sensitivity for the rod-efficient blue stimuli is consistent with recordings of rod signals in horizontal cells of cat retina (Nelson, 1977; Lankheet et al., 1996a). The average sensitivity of rod input to macaque H1 cells (Table 1) was about twice that of rod input sensitivities measured in cat horizontal cells (Nelson, 1977; Lankheet et al., 1996a). It is not clear whether this is a small but real species difference, or if it may be due to differences in experimental protocols.

Second, rod responses in cat horizontal cells (Lankheet et al., 1996b) and responses of macaque rod photoreceptors (Schneeweis & Schnapf, 1995) are slow near threshold and speed up with increasing light intensities. Under dark adapted but not light adapted conditions, the dynamics of the threshold responses of H1 cells to our blue stimuli were much slower than to the red stimuli (Fig. 5e), indicating that the dark adapted near-threshold responses to the blue LED were due to rod input while threshold responses to the red LED were dominated by the relatively fast cone input (Fig. 5b).

Third, the dark adapted responses to blue stimuli of intermediate and higher intensities had a prominent slow off component (Figs 3b and 5e). In cat horizontal cells, this hyperpolarizing slow component, or after-ef-

fect, has been shown to originate in rods (Steinberg, 1969a; Nelson et al., 1976; Nelson, 1977). Lastly, the dark adapted H1 cell responses to the blue LED at intensities above threshold for cone input had a prominent transient at stimulus onset that was not present in dark adapted responses to the red LED (Figs 2b and 3b). Macaque rod photoreceptors also show an initial transient component in response to high intensity light stimuli (Schneeweis & Schnapf, 1995).

Estimations of the passive cable properties of the long, thin axons of horizontal cells exclude a significant input to the cell body from the rod-contacting axon terminal (Nelson et al., 1975). If, however, the H1 axon terminal were the source of rod signals in the cell body, one would expect the rod and cone mediated receptive fields to be widely displaced since the H1 cell axon terminal is displaced from the cell body by up to millimeters (Rodieck, 1988). Alternatively, if the H1 axon terminals are strongly coupled and displaced in random directions compared to the cell body, the rod receptive field may not be displaced but it will be much larger than the cone receptive field (Kamermans, van Dijk & Spekreijse, 1990). In our recordings from H1 cell bodies, rod and cone mediated receptive fields of dark adapted H1 cells were coextensive and similar in size (Fig. 7), consistent with the Nelson (1977) finding of coextensive rod and cone mediated receptive fields in cat horizontal cells. This finding provides evidence that rod signals in H1 cell bodies in our preparation were transmitted via rod-cone gap junctions.

4.2. Sensitivity and dynamics of the H1 rod signal: implications for two rod mechanisms

Psychophysical measurements of human vision and the electroretinogram make several predictions about the relative sensitivities and temporal properties of the two rod mechanisms. First, the threshold of the signals differs by about 2–3 log units (Conner & MacLeod, 1977; Sharpe & Stockman, 1991; Stockman et al., 1995). Second, for light levels on the order of 1 scotopic troland (about 5 quanta $\mu m^{-2} s^{-1}$ for a wavelength of 507 nm) (Shapley & Enroth-Cugell, 1984) one signal is delayed by about 33 ms compared to the other (Sharpe et al., 1989; Sharpe & Stockman, 1991). Third, the cutoff frequency of the faster signal increases with light level up to an intensity of about 500 quanta $\mu m^{-2} s^{-1}$, at which level it is consistent with a psychophysical flicker fusion frequency of 28 Hz (Conner & MacLeod, 1977). In this section we discuss the evidence that the rod bipolar pathway is sensitive and slow, and the rod-cone pathway is insensitive and fast.

The average sensitivity of rod input in macaque H1 cells was about 1.4 log units greater than the sensitivity of L- cone input (Table 1), much less than would be expected if this pathway contributed to low scotopic vision. Several studies in primate and mammalian retina point to a greater sensitivity in the rod bipolar pathway. Preliminary data on the rod signal recorded in macaque AII amacrine cells showed that these cells respond over a 6 log unit range of stimulus intensity—from low scotopic to high photopic levels (Buck, Stone & Dacey, 1997; Stone, Buck & Dacey, 1997)—suggesting at least 3 log units greater sensitivity in the rod bipolar pathway. In rabbit retina, both rod bipolar cells and AII amacrine cells also respond over a 6 log unit range of intensity, with threshold for both cell types one log unit below threshold for the electroretinogram b-wave (Dacheux & Raviola, 1986). Studies in cat retina have suggested that threshold for rod signals in AII amacrine cells is lower than in the cell bodies of horizontal cells (Nelson, 1977, 1982) and, while cat ganglion cells respond to rod signals over more than a 5 log unit range of intensities (Barlow & Levick, 1969; Shapley & Enroth-Cugell, 1984; Lankheet et al., 1996a), rod activity in cat horizontal cells is detected over a more limited intensity range of about 3 log units (Lankheet et al., 1996a,b). These findings in cat and rabbit, and the present study in macaque retina, support the hypothesis that the rod-cone pathway is less sensitive than the rod bipolar pathway and does not appear to contribute to low scotopic vision.

Our finding that the time to peak of rod mediated responses in macaque H1 cells decreased with increasing stimulus intensity is consistent with Schneeweis and Schnapf (1995) results from recordings of macaque rods. The peak latencies of rod input responses in H1 cells (Fig. 5e) were also very similar to latencies reported for macaque rods (Schneeweis & Schnapf, 1995), suggesting that transmission across the cone-H1 cell synapse does not significantly alter rod response latencies. A comparison of response latencies between the two rod pathways is somewhat difficult, however, because of conflicting evidence on the response latencies of cells in the rod bipolar pathway. ERG studies in cat (Robson & Frishman, 1995) and humans (Hood & Birch, 1996) support the view that rod signals are accelerated at the rod-rod bipolar cell synapse, while Nelson (1982) reported that the rod signal in the rod bipolar pathway is accelerated at the level of the AII amacrine cell in cat retina. On the other hand, measurements of rod bipolar cell and AII amacrine cell responses in rabbit retina suggest a comparable response time course in these two cell types (Dacheux & Raviola, 1986), and other amacrine cell types in the rod bipolar pathway do not seem to speed up the rod response (Nelson & Kolb, 1984, 1985). Although there is at present somewhat conflicting evidence on the response latencies of cells in the rod bipolar pathway, our results indicate that there is no temporal filtering of rod signals at the level of rod–cone gap junctions. It would seem then that differences in response latencies between the two psychophysical rod mechanisms would have to be explained by a speeding up of

rod signals at some postreceptoral stage in the rod–cone pathway. For example, the rod signal may be high-pass filtered at the cone-cone bipolar synapse, providing a basis for the differences in response latencies between the two rod mechanisms.

The rod-mediated temporal frequency response of H1 cells had a cutoff frequency below 10 Hz (Fig. 6). Preliminary data on the rod-mediated temporal frequency response of macaque AII amacrine cells under scotopic conditions showed a cutoff frequency similar to that of H1 cells (Buck et al., 1997). It is possible that retinal processing further along the rod–cone pathway, for example at the cone–cone bipolar cell synapse, could increase the cutoff frequency of the rod signal. A quantitative comparison between the two rod signals using the same stimuli needs to be performed in order to resolve the question of a difference in temporal resolution between the two rod pathways.

In summary, the present data on the sensitivity of rod input in H1 cells are consistent with the hypothesis that the primate rod–cone pathway is less sensitive than the rod bipolar pathway. Our results on the response latencies of rod signals in H1 cells suggest that there is no temporal filtering of rod signals at the level of rod–cone gap junctions. Furthermore, the temporal resolution of H1 cells appears to be similar to that of macaque AII cells. These two results leave unanswered questions as to whether the rod–cone pathway is faster and whether there is a difference in temporal resolution between the two pathways. To further explore the hypothesis that the rod bipolar pathway is more sensitive and slower than the rod–cone pathway, it will be necessary to measure rod signals in the rod bipolar pathway, that is, in the rod bipolar cell itself or in the AII amacrine cell. Here we predict that: (1) the sensitivity (gain) of the rod signal will be as much as 3 log units higher; (2) the latency of the signal will be about 30 ms longer (for intensities of 5–10 quanta $\mu m^{-2}\ s^{-1}$); and (3) the cutoff frequency at intensities above 10 quanta $\mu m^{-2}\ s^{-1}$ will be considerably lower. Another locus for exploring the rod signal in the rod–cone pathway is the cone bipolar cell. However, since rod signals from both pathways converge in the cone bipolar cell, it would be potentially difficult to sort out the two pathways. Rod signals from the two pathways have been distinguished in bipolar cells in the human electroretinogram (Stockman et al., 1995), so the possibility remains that experiments like this may be done at the single cell level.

Acknowledgements

Supported by NIH grants EY06678 (DMD), EY03221 (SLB), EYO1730 (Vision Research Core) and RR00166 to the Regional Primate Research Center at the University of Washington. Toni Haun and Keith Boro provided technical assistance. Joel Pokorny and Vivianne Smith offered helpful comments on the manuscript. We are also grateful to Joel Pokorny, Vivianne Smith, and Barry Lee for help in setting up the LED-based stimulus and for designing data acquisition and analysis software. DMD warmly thanks Kate Mulligan for her continued support.

References

Barlow, H. B., & Levick, W. R. (1969). Three factors limiting the reliable detection of light by retinal ganglion cells of the cat. *Journal of Physiology*, *200*, 1–24.

Baylor, D. A., Nunn, B. J., & Schnapf, J. L. (1984). The photocurrent, noise and spectral sensitivity of rods of the monkey *Macaca fascicularis*. *Journal of Physiology*, *357*, 575–607.

Baylor, D. A., Nunn, B. J., & Schnapf, J. L. (1987). Spectral sensitivity of cones of the monkey *Macaca fascicularis*. *Journal of Physiology*, *390*, 145–160.

Blakemore, C. B., & Rushton, W. A. H. (1998). Dark adaptation and increment threshold in a rod monochromat. *Journal of Physiology*, *181*, 612–628.

Buck, S. (1989). A model of dual rod pathways. *Journal of the Optical Society of America Digest Series*, *18*, 225–226.

Buck, S. L., Stone, S., & Dacey, D. M. (1997). Physiology of rod-cone interactions in the AII amacrine cell in macaque monkey retina (supplement, abstract). *Investigative Ophthalmology and Visual Science*, *38*, S708.

Conner, J. D., & MacLeod, D. I. (1977). Rod photoreceptors detect rapid flicker. *Science*, *195*, 698–699.

Conner, J. D. (1982). The temporal properties of rod vision. *Journal of Physiology*, *332*, 139–155.

Dacey, D. M., & Lee, B. B. (1994). The blue-ON opponent pathway in primate retina originates from a distinct bistratified ganglion cell type. *Nature*, *367*, 731–735.

Dacey, D. M., Lee, B. B., Stafford, D. K., Pokorny, J., & Smith, V. C. (1996). Horizontal cells of the primate retina: cone specificity without spectral opponency. *Science*, *271*, 656–659.

Dacheux, R. F., & Raviola, E. (1986). The rod pathway in the rabbit retina. A depolarizing bipolar and amacrine cell. *Journal of Neuroscience*, *6*, 331–345.

Famiglietti, E. V., & Kolb, H. (1975). A bistratified amacrine cell and synaptic circuitry in the inner plexiform layer of the retina. *Brain Research*, *84*, 293–300.

Hecht, S., Shlaer, S., Smith, E. L., Haig, C., & Peskin, J. C. (1938). The visual function of a completely colorblind person. *American Journal of Physiology*, *123*, 94–95.

Hecht, S., Shlaer, S., Smith, E. L., Haig, C., & Peskin, J. C. (1948). The visual functions of the complete colorblind. *Journal of General Physiology*, *31*, 459–472.

Heimer, C. V., & Taylor, C. E. D. (1974). Improved mountant for immunofluorescent preparations. *Journal of Clinical Pathology*, *27*, 254–256.

Hess, R. F., & Nordby, K. (1986). Spatial and temporal limits of vision in the achromat. *Journal of Physiology*, *371*, 365–385.

Hood, D. C., & Birch, D. G. (1996). b wave of the scotopic (rod) electroretinogram as a measure of the activity of human on-bipolar cells. *Journal of the Optical Society of America*, *13*, 623–633.

Kamermans, M., van Dijk, B. W., & Spekreijse, H. (1990). Interaction between the soma and the axon terminal of horizontal cells in carp retina. *Vision Research*, *30*(7), 1011–1016.

Knight, R., & Buck, S. (1993). Cone pathways and the $\pi 0$ and $\pi 0'$ rod mechanisms. *Vision Research*, *33*, 2203–2213.

Kolb, H. (1970). Organization of the outer plexiform layer of the primate retina: electron microscopy of golgi-impregnated cells. *Philosophical Transactions of the Royal Society of London, Series B: Biological Sciences*, *B258*, 261–283.

Kolb, H., & Famiglietti, E. V. (1974). Rod and cone pathways in the inner plexiform layer of cat retina. *Science*, *186*, 47–49.

Lankheet, M. J. M., Rowe, M. H., van Wezel, R. J. A., & van de Grind, W. A. (1996a). Horizontal cell sensitivity in the cat retina during prolonged dark adaptation. *Visual Neuroscience*, *13*, 885–896.

Lankheet, M. J. M., Rowe, M. H., van Wezel, R. J. A., & van de Grind, W. A. (1996b). Spatial and temporal properties of cat horizontal cells after prolonged dark adaptation. *Vision Research*, *36*, 3955–3967.

Muller, F., Wässle, H., & Voigt, T. (1988). Pharmacological modulation of the rod pathway in the cat retina. *Journal of Neurophysiology*, *59*, 1657–1672.

Nelson, R., Lutzow, A. V., Kolb, H., & Gouras, P. (1975). Horizontal cells in cat retina with independent dendritic systems. *Science*, *189*, 137–139.

Nelson, R., Kolb, H., Famiglietti, E. V., & Gouras, P. (1976). Neural responses in the rod and cone systems of the cat retina: intracellular records and procion stains. *Investigative Ophthalmology and Visual Science*, *15*, 946–953.

Nelson, R. (1977). Cat cones have rod input: a comparison of the response properties of cones and horizontal cell bodies in the retina of the cat. *Journal of Comparative Neurology*, *172*, 109–136.

Nelson, R. (1982). AII amacrine cells quicken time course of rod signals in the cat retina. *Journal of Neurophysiology*, *47*(5), 928–947.

Nelson, R., & Kolb, H. (1984). Amacrine cells in scotopic vision. *Ophthalmic Research*, *16*, 21–26.

Nelson, R., & Kolb, H. (1985). A17: a broad-field amacrine cell in the rod system of the cat retina. *Journal of Physiology* (*London*), *54*, 592–613.

Raviola, E., & Gilula, N. B. (1973). Gap junctions between photoreceptor cells in the vertebrate retina. *Proceedings of the National Academy of Sciences USA*, *70*, 1677–1681.

Robson, J. G., & Frishman, L. J. (1995). Response linearity and kinetics of the cat retina: the bipolar cell component of the dark-adapted electroretinogram. *Visual Neuroscience*, *12*, 837–850.

Rodieck, R. W. (1988). The primate retina. In H. D. Steklis, *Comparative primate biology. Neurosciences*, vol. 4 (pp. 203–278). New York: Alan R. Liss, Inc.

Schneeweis, D. M., & Schnapf, J. L. (1995). Photovoltage of rods and cones in the macaque retina. *Science*, *268*, 1053–1056.

Shapley, R., & Enroth-Cugell, C. (1984). Visual adaptation and retinal gain controls. *Progress in Retinal Research*, *4*, 263–346.

Sharpe, L. T., Stockman, A., & MacLeod, D. I. (1989). Rod flicker perception: scotopic duality, phase lags and destructive interference. *Vision Research*, *29*, 1539–1559.

Sharpe, L. T., & Stockman, A. (1991). Dual rod pathways. In A. Valberg, & B. B. Lee, *From pigments to perception* (pp. 53–66). New York: Plenum Press.

Smith, R. G., Freed, M. A., & Sterling, P. (1986). Microcircuitry of the dark-adapted cat retina: functional architecture of the rod–cone network. *Journal of Neuroscience*, *6*, 3505–3517.

Stafford, D. K., & Dacey, D. M. (1997). Physiology of the A1 amacrine cell: a spiking, axon bearing interneuron of the macaque monkey retina. *Visual Neuroscience*, *14*, 507–522.

Steinberg, R. H. (1969a). Rod and cone contributions to S-potentials from the cat retina. *Vision Research*, *9*, 1319–1329.

Steinberg, R. H. (1969b). Rod-cone interaction in S-potentials from the cat retina. *Journal of Physiology* (*London*), *9*, 1331–1344.

Steinberg, R. H. (1969c). The rod after-effect in S-potentials from the cat retina. *Vision Research*, *9*, 1345–1355.

Stockman, A., Sharpe, L. T., Rüther, K., & Nordby, K. (1995). Two signals in the human rod visual system: a model based on electrophysiological data. *Visual Neuroscience*, *12*, 951–970.

Stone, S., Buck, S. L., & Dacey, D. M. (1997). Pharmacological dissection of rod and cone bipolar input to the AII amacrine in macaque retina (supplement, abstract). *Investigative Ophthalmology and Visual Science*, *38*, S689.

Strettoi, E., Dacheux, R. F., & Raviola, E. (1994). Cone bipolar cells as interneurons in the rod pathway of the rabbit retina. *Journal of Comparative Neurology*, *347*, 139–149.

Strettoi, E., Raviola, E., & Dacheux, R. F. (1992). Synaptic connections of the narrow-field, bistratified rod amacrine cell (AII) in the rabbit retina. *Journal of Comparative Neurology*, *325*, 152–168.